The use of three-dimensional NMR in structural studies of oligosaccharides

ARTICLE *in* JOURNAL OF THE AMERICAN CHEMICAL SOCIETY · JANUARY 1989

Impact Factor: 12.11 · DOI: 10.1021/ja00184a078

and cross peaks corresponding to H1 and another proton (H3) that is scalar coupled to H2. This procedure is continued by selecting the protons that are scalar coupled to H3 from the plane (C3) that displays the proper pattern of proton signals (diagonal peak at H3, cross peak at H2). Ambiguities in the assignments which arise from protons resonating at the same frequency can be resolved in this experiment by editing the COSY data by the ^{13}C frequencies. For example, although the 1 and 3 protons of ring A have nearly identical chemical shifts, the shifts of the attached carbons (C1 and C3) are different. Thus, as shown in column 1 of Figure 2, the COSY responses involving the degenerate signals of H1 and H3 can be distinguished by their location in different planes (C1, H6-H1-H2; C3,H4-H3-H2).

Analogous to a two-dimensional heteronuclear relay experiment,[10] the 3D HMQC-COSY experiment provides relay information by correlating the chemical shifts of a carbon, the attached proton(s), and their scalar coupled partners. In contrast to the heteronuclear relay experiment, however, the 3D experiment uniquely defines the frequency of the relay spin.[2,3] This is important in cases where ^{13}C signals overlap such as C3 and C4 in ring B of kanamycin A. Since the relay spins (H3, H4) are uniquely defined in ω_2 in the 3D experiment, the H2-H3-H4 and H3-H4-H5 connectivity patterns can easily be distinguished (Figure 2).

In summary, heteronuclear 3D NMR spectroscopy is a useful method for resolving spectral overlap in all frequency domains. This is important for assigning spectra and elucidating the structures of complicated molecules. In addition, the increase in resolution afforded by this technique will help to automate peak-picking and assignment procedures and facilitate the extraction of J couplings (HMQC-COSY) and quantitative NOE information (HMQC-NOESY) used in the determination of three-dimensional structures.

Acknowledgment. We thank Dr. J. McAlpine for the sample of kanamycin A.

(10) (a) Bolton, P. H. *J. Magn. Reson.* **1982**, *48*, 336. (b) Bolton, P. H.; Bodenhausen, G. *Chem. Phys. Lett.* **1982**, *89*, 139.

The Use of 3D NMR in Structural Studies of Oligosaccharides

G. W. Vuister, P. de Waard, R. Boelens,
J. F. G. Vliegenthart, and R. Kaptein*

Department of Chemistry, University of Utrecht
Padualaan 8, 3584 CH Utrecht, The Netherlands

Received September 12, 1988

The three-dimensional structures of oligosaccharides derived from glycoproteins can be specified by the conformation of the glycosidic linkages, in particular the torsion angles ϕ and ψ and the additional torsion angle ω for 1-6 linkages.[1] Two-dimensional NOE spectra can provide interresidue proton distances, from which these torsion angles can be estimated. However, the small chemical shift dispersion of the sugar skeleton protons presents a major problem. In particular in the bulk region between 3 and 4 ppm there is a serious overlap of resonances. Often assignments can still be made in this region by multiple relayed COSY[2] or by 1D or 2D homonuclear Hartmann-Hahn (HOHAHA) experiments[3] by using the shift dispersion of the anomeric protons. However, the NOE's involving protons of the bulk region would still be difficult to interpret.

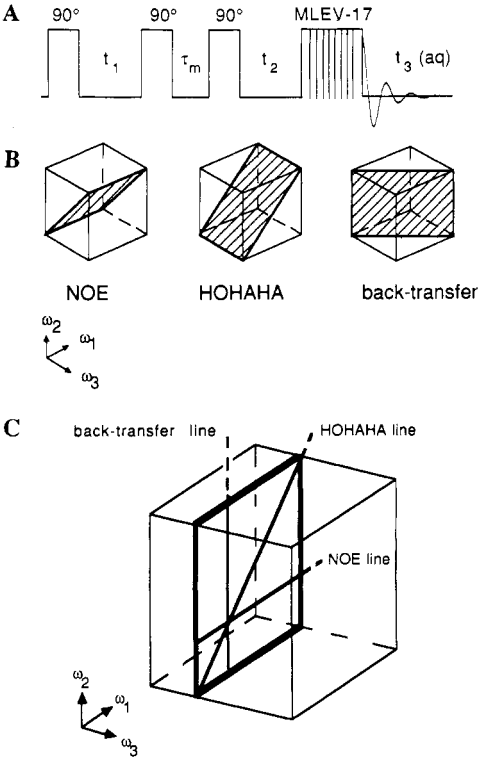

Figure 1. Nonselective 3D NOE-HOHAHA experiment. (A) Pulse sequence. (B) Cross diagonal planes in a 3D NOE-HOHAHA spectrum showing the NOE plane ($\omega_2 = \omega_3$), HOHAHA plane ($\omega_1 = \omega_2$), and back-transfer plane ($\omega_1 = \omega_3$). (C) Cross section perpendicular to the ω_3 axis. NOE, HOHAHA, and back-transfer lines result from intersection with the three planes indicated in part B.

The spectral resolution of the NMR methods can be increased by adding a third frequency domain.[4] Here we shall give an example of the application of 3D NMR to the diantennery asparagine-linked oligosaccharide **1**.

We will show that useful information on protons resonating in the bulk region can be extracted from a nonselective 3D NOE-HOHAHA experiment,[4f] which covers the full chemical shift range in all three dimensions.

The 3D NOE-HOHAHA can be visualized as a combination of a 2D NOE and a 2D HOHAHA or TOCSY experiment. The pulse sequence is shown in Figure 1A. The free induction decays (FIDs) are recorded in t_3 as a function of two independent evolution times t_1 and t_2. After 3D Fourier transformation of the FID's, the 3D frequency space can be represented in a cube with axes ω_1, ω_2, and ω_3. In the 3D spectrum obtained in this way a body diagonal ($\omega_1 = \omega_2 = \omega_3$) can be identified, containing magnetization not transferred during any of the mixing periods. Furthermore, intensity accumulates on the three cross-diagonal planes as shown in Figure 1B. The plane $\omega_2 = \omega_3$ (NOE plane) contains the magnetization transferred only during the NOE mixing period, whereas the plane $\omega_1 = \omega_2$ (HOHAHA plane) contains the magnetization transferred only during the isotropic mixing period of the MLEV-17 sequence. Finally, the plane $\omega_1 = \omega_3$ (back-transfer plane) contains magnetization transferred during the NOE mixing period from spin a to spin b and then

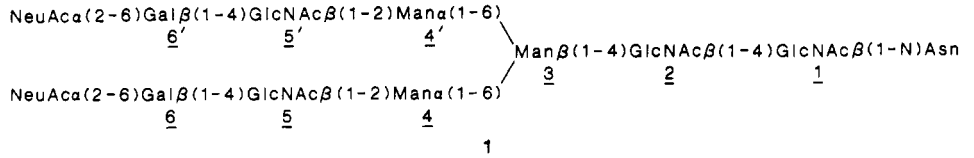

1

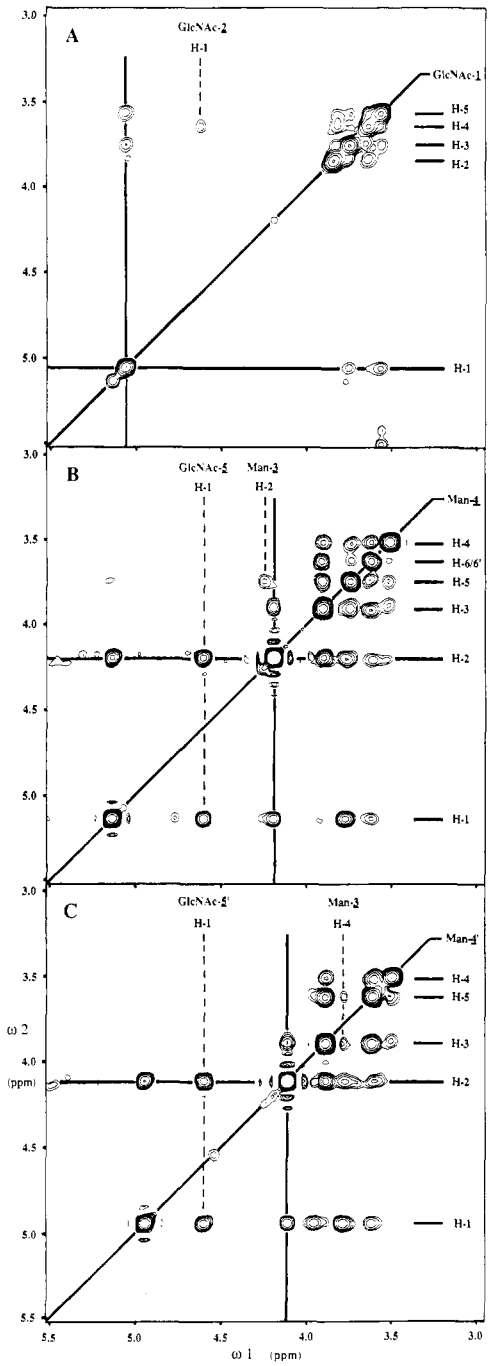

Figure 2. Cross sections perpendicular to the ω_3 axis of the 3D NOE–HOHAHA ^{1}H spectrum of a 20 mM solution of **1** in D_2O at 304 K and pH = 7. Cross sections are shown at the ω_3 resonance positions of GlcNAc-1 H-1 (A), Man-4 H-2 (B), and Man-4′ H-2 (C). The NOE, HOHAHA, and back-transfer lines are indicated. The phase-sensitive spectrum was recorded at 500 MHz on a Bruker AM500 spectrometer by using a phase cycle of four steps on the pulse after the NOE mixing period. Combined with a phase cycle of two steps for axial peak suppression this yielded 8 scans for each FID. Acquisition was preceded by two dummy scans. Positive and negative frequencies in ω_1 and ω_2 were separated by independent TPPI on the preparation pulse and the pulse prior to the t_2 evolution period. FIDs were recorded at a size of 1 K. This was repeated independently for 144 incremental t_1 and t_2 values, resulting in a total measuring time of approximately 63 h. During the relaxation delay of 0.45 s the HDO resonance was suppressed by radiation. Spectral width in all three time domains was 2272.7 Hz. The NOE mixing time was 0.35 s. Isotropic mixing was induced by an MLEV-17 sequence of 94 ms with trim pulses at the beginning and the end. Data were zerofilled twice in the t_1 and t_2 domain before Fourier transformation. Cosine bell windows were used in all three time domains. The resulting data set of 256 × 256 × 512 points was base line corrected in all frequency domains by a third-order polynomial fit.

back to spin *a* during the isotropic mixing period.

For the analysis of 3D NMR spectra, cross-sectional planes perpendicular to the ω_3 axis (called ω_3 cross sections) can be used (see Figure 1C). The three special planes of Figure 1B intersect this cross section at the three lines indicated as NOE, HOHAHA, and back-transfer lines. These lines intersect all at one point which lies on the body diagonal of the cube. Cross-diagonal peaks lying on the NOE or HOHAHA lines in the cross section taken at $\omega_3 = \omega_a$ represent single magnetization transfer (by NOE or isotropic mixing, respectively) to a proton *a*. These lines are therefore similar to columns in 2D NOE or 2D HOHAHA spectra. All other cross peaks are due to double magnetization transfer.

Figure 2 shows three ω_3 cross sections of the 3D spectrum of **1**. In Figure 2A a cross section of H-1 of GlcNAc-1 at 5.05 ppm shows an example of the unambiguous assignment of NOE's in 3D NMR. The HOHAHA line (diagonal) shows the *J*-coupled connectivities to other protons of the same residue. The two cross peaks on the NOE line (horizontal) are also found on the back-transfer line (vertical), indicating two intraresidue NOE's between H-1 and the H-3 and H-5 protons located on the same side of the sugar ring. This is confirmed by the 3D cross peak between H-3 and H-5. The remaining cross peaks on the HOHAHA line are assigned to the H-2 and H-4 protons on the basis of earlier 2D HOHAHA experiments with different isotropic mixing times (unpublished results). These resonances also have an intraresidue 3D NOE cross peak. On the horizontal line at the ω_2 position of the H-4 of GlcNAc-1 the indicated cross peak can be easily assigned as an NOE to the GlcNAc-2 anomeric proton, confirming the 1–4 linkage between these residues. In 2D NOE spectra the NOE between the anomeric GlcNAc-2 H-1 and the GlcNAc-1 H-4 hidden in the bulk region could not have been unambiguously assigned due to overlap of the latter resonance with other signals. However, in 3D NMR by the double magnetization transfer (NOE and HOHAHA) this NOE can be correlated to the uniquely assigned anomeric proton of GlcNAc-1.

Another example is given in Figure 2B showing a ω_3 cross section of Man-4 H-2 at 4.19 ppm. The cross peaks on the HOHAHA line of this residue were assigned by comparing the cross sections at the Man-4 H-2 frequency with that of Man-4 H-1 (data not shown). Interresidue NOE cross peaks between the anomeric proton of GlcNAc-5 and the H-1 and H-2 protons of Man-4 are present. The presence of an NOE between Man-4 H-5 and Man-3 H-2 has been the subject of extensive discussion. The existence of this NOE was disputed by Homans et al.,[5] but it was finally proved by Cumming et al. in an elaborated study with a synthesized specifically deuterated trimannoside.[6] In the 3D spectrum of the complete biantennery structure this NOE effect is found in a direct way in Figure 2B.

An example of 3D NOE cross peaks within the bulk region is given in Figure 2C, which shows a cross section at the Man-4′ H-2 frequency at 4.11 ppm. In this figure 3D cross peaks between the H-3 and H-5 protons of Man-4′ and another resonance at 3.77 ppm within the bulk region are observed. The absence of a cross peak on the HOHAHA line at this frequency indicates that this

(1) Carver, J. P.; Brisson, J. R. *Biology of Carbohydrates*; Wiley: New York, 1984; pp 289–331.
(2) Homans, S. W.; Dwek, R. A.; Fernandes, D. L.; Rademacher, T. W. *Proc. Natl. Acad. Sci. U.S.A.* **1984**, *81*, 6286–6289.
(3) (a) Davis, D. G.; Bax, A. *J. Am. Chem. Soc.* **1985**, *107*, 7198–7199. (b) Homans, S. W.; Dwek, R. A.; Boyd, J.; Soffe, N.; Rademacher, T. W. *Proc. Natl. Acad. Sci. U.S.A.* **1987**, *84*, 1202–1205. (c) Inagaki, F.; Kodama, C.; Suzuki, M.; Suzuki, A. *FEBS Lett.* **1987**, *219*, 45–50.
(4) (a) Vuister, G. W.; Boelens, R. *J. Magn. Reson.* **1987**, *73*, 328–333. (b) Griesinger, C.; Sørensen, O. W.; Ernst, R. R. *J. Magn. Reson.* **1987**, *73*, 574–579. (c) Griesinger, C.; Sørensen, O. W.; Ernst, R. R. *J. Am. Chem. Soc.* **1987**, *109*, 7227–7228. (d) Oschkinat, H.; Griesinger, C.; Kraulis, P. J.; Sørensen, O. W.; Ernst, R. R. *Nature* **1988**, 374–376. (e) Fesik, S. W.; Zuiderweg, E. R. P. *J. Magn. Reson.* **1988**, 588–593. (f) Vuister, G. W.; Boelens, R.; Kaptein, R. *J. Magn. Reson.* **1988**, *80*, 176–185.
(5) Homans, S. W.; Dwek, R. A.; Fernandes, D. L.; Rademacher, T. W. *FEBS Lett.* **1983**, *164*, 231–235.
(6) Cumming, D. A.; Dime, D. S.; Grey, A. A.; Krepinsky, J. J.; Carver, J. P. *J. Biol. Chem.* **1986**, *261*, 3208–3213.
256 × 256 × 512 points was base line corrected in all frequency domains by a third-order polynomial fit.

resonance does not belong to a proton of Man-4'. Inspection of the structure of **1** shows that a likely candidate is the H-4 of the neighboring Man-3. The proximity of the Man-3 H-4 to the Man-4' H-3 and H-5 atoms would confirm the existence of a 1-6 linkage in which the conformation with (ϕ,ψ,ω) = (-60°,180°,180°) must be present.

The present work illustrates the usefulness of 3D NMR techniques in structure elucidations of complicated oligosaccharides. The examples of Figure 2, parts A and B, show that unique asssignments of NOE's can be made, which would have required certain assumptions in 2D NMR. Furthermore the observation of NOE's between protons within the bulk region would be very difficult in 2D NMR.

Acknowledgment. This work was supported by the Netherlands Foundation for Chemical Research (SON) with financial aid from the Netherlands Foundation of Scientific Research (NWO). Thanks to Profs. G. Spik and J. Montreuil, Université des Sciences et Techniques de Lille Flandres Artois, France, for the gift of the diantennery compound.

$[Mn_{10}O_{14}\{N(CH_2CH_2NH_2)_3\}_6]^{8+}$: A Mixed-Valence Polyoxomanganese Polycation Possessing Structural Similarities to Naturally Occurring Layered Manganese Oxides

Karl S. Hagen and William H. Armstrong*

Department of Chemistry, University of California Berkeley, California 94720

Marilyn M. Olmstead

Department of Chemistry, University of California Davis, California 95616

Received April 5, 1988

Early transition element polyoxoanions have received a great deal of attention for many years,[1,2] in part because of the analogy between these compounds and extended metal oxide materials. As a consequence, many discrete polyoxo anionic aggregates of V(V), Nb(V), Ta(V), Mo(VI), and W(VI) have been characterized. In contrast, there are relatively few well-defined polyoxo/hydroxo complexes of manganese and iron. This situation is presumably a consequence of the difficulty in controlling the hydrolytic or oxidative aggregation chemistry of these latter elements. High-nuclearity[3] carboxylate-bridged polyoxo Mn and Fe complexes, including those with 9,[4,5] 11,[6] and 12[7] metal atoms, have been reported recently. In addition, hydrolysis of Fe(tacn)Cl_3 yields an octanuclear complex.[8] Our interest in manganese oxo chemistry originates not only from the desire to understand and control the formation of soluble polyoxo aggregates as analogues of metal oxide surfaces but also because the oxygen-evolving complex of photosystem II most likely consists of a polynuclear manganese-oxo complex.[9] Herein we report the synthesis, isolation, and structure of a discrete polyoxomanganese cation, $[Mn_{10}O_{14}(tren)_6]^{8+}$ (**1**), which resembles in some respects the layered structures[10] of naturally occurring manganese oxide minerals chalcophanite ($ZnMn_3O_7\cdot 3H_2O$),[11a,12] and lithiophorite ($(Al,Li)MnO_2(OH)_2$).[11b,12]

In a previous report,[13] we described the synthesis of a binuclear manganese complex obtained by controlled air oxidation of a solution containing $Mn(CF_3SO_3)_2$ and tren. In that case, air exposure was terminated after 2 h to yield a green complex, $[Mn_2O_2(tren)_2](CF_3SO_3)_3$ (**2**). It was noted that further air oxidation resulted in a brown solution. Characterization of a brown species from this latter solution constitutes the basis of this communication. The synthesis of **1** is initiated by dissolving 1.6 g of $Mn(CF_3SO_3)_2\cdot 2MeCN$ and 0.64 g of tren in 10 mL of MeCN under N_2. After overnight exposure to the air, 5 mL of Et_2O was carefully layered on top of the MeCN solution. The crystals of $\mathbf{1}(CF_3SO_3)_8\cdot 6MeCN$ that deposit over 3 days lose solvent rapidly when removed from the mother liquor. However, they were suitable for X-ray diffraction experiments,[14] provided crystal mounting and data collection were carried out at low temperature in order to prevent loss of MeCN from the crystal lattice. The remaining crystals were collected and washed with Et_2O and dried in vacuo to yield 0.49 g of product[15] (47% yield) which analyzes as the desolvated cluster.

The centrosymmetric structure of **1** is shown from two perspectives in Figure 1.[16] On the basis of charge considerations, there are four Mn(III) and six Mn(IV) atoms in the cation. As is the case for other trapped valence manganese complexes **2**,[13] $[Mn_4O_3Cl_6(HIm)(CH_3COO)_3]^{2+}$ (**3**),[17] and the dodecanuclear carboxylate species $[Mn_{12}O_{12}(CH_3COO]_{16}(H_2O)_4]$ (**4**);[7] for example, Mn(III) atoms can be identified by the presence of axial bond distances which are elongated due to Jahn-Teller distortions. Thus, Mn(3) and Mn(5),[18] which have long Mn-N distances of 2.291 (2), 2.287 (2), and 2.283 (2) Å are assigned as Mn(III) ions. In contrast, the longest Mn-N distance for Mn(4) is 2.065 (3) Å and is assigned as Mn(IV) along with the remaining Mn atoms, Mn(1) and Mn(2). Three types of bridging oxo groups are present in the structure, including six doubly bridging atoms (O(5), O(6), O(7)) and two types of triply bridging oxo atoms. Of the eight μ_3-oxo bridges, four (O(3), O(4)) have a "t-shaped" geometry similar to that found in $[Fe_3O(TIEO)_2(O_2CPh)_2Cl_3]$.[5,19] The remaining four oxo groups (O(1), O(2)) are in sites of near trigonal microsymmetry and well out of the plane of the three manganese atoms to which they are attached. Compounds **3** and **4** have similar nonplanar μ_3-oxo bridges.

(1) Day, V. W.; Klemperer, W. G. *Science* **1985**, *228*, 533-541.
(2) Pope, M. T. *Heteropoly and Isopoly Oxometalates*; Springer-Verlag: Heidelberg, 1983.
(3) For the purpose of this discussion, "high-nuclearity complexes" are defined as those with eight or more metal atoms.
(4) $[Mn_9O_4(O_2CPh)_8(salH)_2(pyr)_4]$:[5] Christmas, C.; Vincent, J. B.; Chang, H.-R.; Huffman, J. C.; Christou, G.; Hendrickson, D. N. *J. Am. Chem. Soc.* **1988**, *110*, 823-830.
(5) Abbreviations used: $salH_2$, salicylic acid; pyr, pyridine; tacn, 1,4,7-triazacyclononane; tren, $N(CH_2CH_2NH_2)_3$; HIm, imidazole; TIEO, 1,1,2-tris(*N*-methylimidazol-2-yl)-1-hydroxyethane.
(6) $[Fe_{11}O_6(OH)_6(O_2CPh)_{15}]$: Gorun, S. M.; Papaefthymiou, G. C.; Frankel, R. B.; Lippard, S. J. *J. Am. Chem. Soc.* **1987**, *109*, 3337-3348.
(7) $[Mn_{12}O_{12}(H_2O)_4(O_2CCH_3)_{16}]$: Lis, T. *Acta Crystallogr.* **1980**, *B36*, 2042-2046.
(8) $[Fe_8O_2(OH)_{12}(tacn)_6]^{8+}$: Wieghardt, K.; Pohl, K.; Jibril, I.; Huttner, G. *Angew. Chem., Int. Ed. Engl.* **1984**, *23*, 77-78.
(9) (a) Dismukes, G. *Photochem. Photobiol.* **1986**, *43*, 99-115. (b) Govindjee; Kambara, T.; Coleman, W. *Photochem. Photobiol.* **1985**, *42*, 187-210. (c) Babcock, G. T. In *New Comprehensive Biochemistry: Photosynthesis*; Amesz, J., Ed.; Elsevier: Amsterdam, 1987; pp 125-158.
(10) Raveau, B. *Rev. Inorg. Chem.* **1987**, *9*, 37-64.
(11) (a) Wadsley, A. D. *Acta Crystallogr.* **1955**, *8*, 165-172. (b) Wadsley, A. D. *Acta Crystallogr.* **1952**, *5*, 676-680.
(12) Wells, A. F. *Structural Inorganic Chemistry*, 5th ed.; Clarendon Press: Oxford, 1984; pp 553-556.
(13) Hagen, K. S.; Armstrong, W. H.; Hope, H. *Inorg. Chem.* **1988**, *27*, 967-969.
(14) X-ray analysis: The compound $[Mn_{10}O_{14}(tren)_6](CF_3SO_3)_8\cdot 6MeCN$ crystallizes in the triclinic system space group $P\bar{1}$, with a = 15.658 (7) Å, b = 15.681 (3) Å, c = 15.557 (3) Å, α = 115.80 (1)°, β = 92.26 (2)°, γ = 119.21 (2)°, V = 2842 Å^3, ρ(calcd) = 1.756 g cm^{-3}, and Z = 1. With the use of 8003 reflections collected at 163 K with Mo Kα (λ = 0.71073 Å) radiation out to 2θ = 45° on a single-crystal X-ray diffractometer, the structure was solved by a combination of Patterson and direct methods (SHELXS 86) and difference Fourier methods and refined to R (R_w) values of 3.6% (4.7%).
(15) Anal. Calcd for $C_{44}H_{108}F_{24}Mn_{10}N_{24}O_{38}S_8$: C, 18.58; H, 3.83; N, 11.82. Found: C, 18.17; H, 3.70; N, 11.58.
(16) Selected bond distances and angles (a full listing is provided as Supplementary Material): Mn(1)-O(1) 1.980 (2), Mn(1)-O(2) 1.874 (2), Mn(1)-O(3) 1.914 (2), Mn(1)-O(5) 1.804 (2), Mn(1)-O(1') 1.898 (2), Mn(1)-N(21) 2.058 (2), Mn(3)-O(2) 1.918 (2), Mn(3)-O(5) 1.828 (2), Mn(3)-O(4') 2.136 (2), Mn(3)-N(11) 2.291 (2), Mn(3)-N(31) 2.070 (3), Mn(3)-N(41) 2.083 (2), Mn(1)-O(1)-Mn(1') 96.7 (1), Mn(1)-O(1)-Mn(2) 93.95 (8), Mn(2)-O(1)-Mn(1') 96.89 (6), Mn(1)-O(3)-Mn(2) 99.4 (1), Mn(1)-O(3)-Mn(5) 165.4 (2), Mn(2)-O(3)-Mn(5) 92.51 (9), Mn(1)-O(5)-Mn(3) 98.0 (1), Mn(2)-O(6)-Mn(5) 96.6 (1).
(17) Bashkin, J. S.; Chang, H.-R.; Streib, W. E.; Huffman, J. C.; Hendrickson, D. N.; Christou, G. *J. Am. Chem. Soc.* **1987**, *109*, 6502-6504.
(18) Only the atoms in the assymetric unit are listed; the others being generated by the inversion center.
(19) Gorun, S. M.; Papaefthymiou, G. C.; Frankel, R. B.; Lippard, S. J. *J. Am. Chem. Soc.* **1987**, *109*, 4244-4255.

0002-7863/89/1511-0774$01.50/0